Soft Monte Carlo Simulation for imprecise probability estimation: A dimension reduction-based approach

Azam Abdollahi[a,b,*], Hossein Shahraki[c], Matthias G.R. Faes[d], Mohsen Rashki[a]

[a] *University of Sistan and Baluchestan, Zahedan, Iran*
[b] *Lakehead University, Ontario, Canada*
[c] *University of Bojnord, Bojnord, Iran*
[d] *Chair for Reliability Engineering, TU Dortmund University, Dortmund, Germany*

Abstract

This paper proposes an efficient solution for solving hybrid reliability problems involving random and interval variables. To meet this aim, using the soft Monte Carlo (SMC) method, a solution is proposed that breaks the random variables space into local 1-D coordinates and then, considers 1-D coordinate as an additional dimension of interval variables. Accordingly, using an optimization in increased interval variables space, the upper and lower bounds of failure probability for each 1-D problem are estimated. In addition, the total failure probabilities are presented as the mathematical expectation of the obtained probability bounds for 1-D coordinates. Then, it is shown that this approach is fit for application of univariate dimension reduction method to reduce the function calls of analysis in the optimization phase. This approach is validated by solving benchmark reliability problems as well as the application of the proposed method for solving real world engineering problems investigated by solving hybrid reliability analysis of reinforced concrete columns. It is shown that the proposed approach efficiently approximates the failure probability bound of problems with moderate nonlinear limit state functions with high accuracy.

Keywords: Hybrid reliability analysis, Failure probability, High-dimension model representation, Imprecise probability, Optimization

1. Introduction

In the analysis and design of most engineering systems, we are faced with different sources of uncertainties, rooted in incomplete/imprecise knowledge or experimental data, measuring errors, various modeling assumptions, operational conditions and, etc. [1] Generally, in engineering applications, these uncertainties can be classified into two major groups as aleatory and epistemic ones which may be simultaneously in existence in many real-world engineering problems [2]. The characterization of both mentioned types of uncertainties with mathematical models is an open field of research in uncertainty quantification (UQ). To describe the aleatory uncertainty in the response of a numerical model subjected to those uncertainties, several uncertainty propagation approaches (known as structural reliability methods) have been proposed by probability models, including the Monte Carlo simulation (MCS) method [3], subset simulation [4, 5] , adaptive Monte Carlo [6], line sampling [7] and importance sampling [8]. In case sufficient data and knowledge are available to the analyst to model the occuring natural variability, it is without discussion that these well-established probabilistic techniques should be applied. However, at the same time, it is important to acknowledge that, especially in engineering practice, such datasets are more often than not unavailable due to constraints on costs, experimental time or material. On top, when considering for instance early design phases where the complete structure has not been dimensioned yet, the uncertainty corresponding to key model quantities is not random in nature, but rather stems from a pure lack of knowledge. In either case, it is questionable to impose a probability density function to the uncertain quantities since this inevitable includes subjective knowledge into the analysis. This knowledge may or may not be adequate. Therefore, in literature, some

*Corresponding author
Email address: azam.abdollahi@pgs.usb.ac.ir (Azam Abdollahi)

techniques such as fuzzy theory [9], P-boxes [10, 11, 12, 13], interval models [14, 15, 16, 17, 18] and evidence theory [19] are utilized to quantify the epistemic uncertainties. From an engineering perspective, these methods should be interpreted as systemized and rigorous approaches to study the effect of these epistemic uncertainties on the result of the probabilistic reliability analyses.

Aimed at providing such estimation of the sensitivity of reliability estimates to epistemic uncertainty, several hybrid reliability analysis (HRA) methods are proposed for handling both aleatory and epistemic uncertainties concurrently [19, 20]. The hybrid reliability analysis with both random and interval variables (HRA-RI) offers a way to compute the upper and lower bounds of failure probability estimation [21, 22]. Among the existing reliability approaches, MCS is a reference method to approximate the upper and lower bounds of failure probability. However, this approach is impractical for time-consuming numerical simulations such as finite element analysis to solve real-world systems. To overcome this drawback, several alternative approaches such as FORM-UUA are proposed which combines unified uncertainty analysis (UUA) method with first order reliability method (FORM) [21]. Although FORM-UUA is efficient to estimate the small failure probabilities, this UQ approach is unable to yield accurate and acceptable results for high-nonlinear or performance functions with multiple design points. Xiao et al. [23] proposed a novel UUA based on mean value first order saddle point approximation (MVFOSPA-UUA). In some cases, MVFOSPA-UUA has two major drawbacks due to the linearization and approximation at the mean value points. However, FORM-based methods [21] contain the linearization error. Consequently, the FORM-based results are more accurate than the MVFOSPA-UUA in cases with requirement to the MPP search. The operator norm theory [24], Non-intrusive Imprecise Stochastic Simulation (NISS) [16] and Bayesian quadrature methods [25] are proposed as efficient and rigorous methods for hybrid uncertainties. Recently, Faes et. al [26] proposed an efficient framework based on operator norm theory to estimate the bounded failure probability for linear systems which are subjected to combination of aleatory and epistemic uncertainties at the same time. This framework is tailored for linear models in conjunction with aleatory uncertainties within linear map, but was also extended to mildly non-linear systems [27]. KSS is an accurate and efficient technique for rare event estimation of engineering problems but the weakness is related to the high-dimensional performance functions. Zhang et al. [22] developed HRA-RI method coupling projection outline based active learning (POAL) and Kriging named POAL-Kriging. They mentioned that the proposed method with Kriging surrogate model may not be proper for high-dimensional performance functions. Adduri and Penmetsa [28] applied response surface method to estimate the implicit limit state functions (LSF) as a closed-form expression in terms of the uncertain variables. This method is applicable for different series or parallel systems with multiple failure criteria. The issue with many of these approaches on top is the sampling-based nature that is integrated in the procedure for integrating the epistemic part of the uncertainty. Especially MCS-based approaches for propagating epistemic uncertainty are problematic from a conceptual and practical standpoint. Conceptually, they assume the epistemic uncertainty to follow a predescribed distribution, which violates the interval paradigms. Practically, they converge to the bounds on the response quantity of interest with the convergence rate of a Monte Carlo simulator, if they converge at all [20].

Table 1 summarizes the reviewed papers related to HRA-RI. As can be seen, studies are classified based on their proposed HRA-RI framework, type of reliability method, and publication time.

Overall, one may note that although several HRA frameworks have been successfully developed to estimate the upper and lower bounds of failure probability, the problem of lack of efficiency still requires to be focused and can be considered a challenging problem in this topic. This paper aims to develop an efficient and accurate method for HRA in context of soft Monte Carlo (SMC) approach [43] and dimension reduction method (DRM) [44, 45] that also abides by the formalisms of the interval paradigm. To properly meet the aim of this study, the remaining parts of this paper are organized as follows: Section 2 briefly explains HRA-RI. Section 3 presents background theory of high dimension model representation. Section 4 describes soft Monte Carlo method and its advantages in comparison to the other reliability methods. Section 5 introduces a robust HRA by employing soft Monte Carlo technique. Section 6 showcases the superiority of the proposed methodology in comparison to other UQ techniques via some numerical examples and real-world engineering applications. Section 7 presents discussions about main findings and finally Section 8 summarizes the major steps in conjunction with main findings of this UQ study.

Table 1: Proposed methods for hybrid reliability analysis with both aleatory uncertainties and interval variables

No.	Proposed HRA-RI	Reliability method	Year [Ref]
1	Framework consists of two components: Direct reliability analysis + Inverse reliability analysis	Gradient-based	2007 [29]
2	Response surface method+ Fast Fourier transforms (FFT)	Gradient- and simulation-based	2007 [28]
3	FORM-UUA: FORM-based Unified Uncertainty Analysis	Gradient-based	2008 [21]
4	Equivalence model: Changing interval variables to the corresponding Uniform distributions	Gradient-based	2012 [30]
5	MVFOSPA-UUA: Unified Uncertainty Analysis (UUA) method based on the Mean Value First Order Saddlepoint Approximation (MVFOSPA)	Gradient-based	2012 [23]
6	ALK-HRA: Active Learning Kriging (ALK) model + MCS	Simulation-based	2014 [31]
7	Two separate loops for interval analysis and probability analysis + Karush–Kuhn–Tucker (KKT) convergency condition	Gradient-based	2015 [32]
8	P-NP-HRA-DS-ERSDM: Probabilistic and Nonprobabilistic Hybrid Reliability Analysis based on Dynamic Substructural Extremum Response Surface Decoupling Method	Gradient-based	2017 [33]
9	POAL-Kriging: POAL + Kriging metamodel where POAL is a novel Projection Outline-based Active Learning method	Simulation-based	2018 [22]
10	KSS: Kriging-based Subset Simulation	Simulation-based	2019 [34]
11	Multiplicative Dimensional Reduction Method (M-DRM) + second-order Taylor expansion + FORM	Gradient-based	2019 [35]
12	UPSORM: Uncertain-Polar Coordinates SORM	Gradient-based	2020 [36]
13	Active learning method based on Kriging model	Simulation-based	2020 [37]
14	Single-loop method where sensitivity factor is computed based on the hybrid conjugate gradient direction and adaptive step length	Gradient-based	2021 [19]
15	Kriging-assisted SSIS where SSIS refers to Subset Simulation Importance Sampling	Simulation-based	2021 [38]
16	FORM + Kriging + Karush-Kuhn-Tucker condition	Gradient- and Simulation-based	2021 [39]
17	Edgeworth series in which using dimension-reduction method and Taylor expansion	Gradient-based	2022 [40]
18	Improved Hasofer–Lind and Rackwitz–Fiessler method	Gradient-based	2022 [41]
19	aAK-MCS: Advanced Adaptive Kriging model-based MCS	Simulation-based	2022 [42]

2. Hybrid reliability analysis with both random and interval variables (HRA-RI)

The failure probability (P_f) estimation for structural reliability problems with random variables is calculated as follows:

$$P_f = \mathbb{P}\left\{g(\boldsymbol{x}) \leq 0\right\} = \int\limits_{g(\boldsymbol{x})\leq 0} f(\boldsymbol{x})\, d\boldsymbol{x}, \tag{1}$$

where $g(\boldsymbol{x})$ indicates a performance function with random variables $\boldsymbol{x}$ and $f(.)$ is the joint probability density function (PDF). It is well-documented in many practical engineering problems [9, 1, 20, 46] that the presence of both random and interval variables is indispensable. Classic probability-based reliability methods in this particular case are not sufficiently capable of dealing with this kind of information, since both sources of uncertainties have to be kept separated meticulously [47].

To overcome this shortcoming, and supplement classical reliability analysis, hybrid reliability analysis methods incorporate both random and interval variables in the performance function, as graphically illustrated in Figure 1. Precisely, this extended performance function is considered as $g(\boldsymbol{x}, \boldsymbol{y})$, where $\boldsymbol{y}^I$ represents m-dimensional vector as:

$$\boldsymbol{y}^I \in \left[\boldsymbol{y}^L, \boldsymbol{y}^U\right] \qquad \boldsymbol{y}^I = \left[\boldsymbol{y}_1^I, \boldsymbol{y}_2^I, ..., \boldsymbol{y}_m^I\right], \tag{2}$$

where $\boldsymbol{y}^L$ and $\boldsymbol{y}^U$ are lower and upper bounds of interval variables $\boldsymbol{y}$. In this essence, the failure probability can be defined in an interval style due to existence of interval variables as:

$$\begin{aligned} P_f^{min} &= \mathbb{P}\left\{\max_{\boldsymbol{y}^L<\boldsymbol{y}<\boldsymbol{y}^U} g(\boldsymbol{x},\boldsymbol{y}) \leq 0\right\} = \int_{\max\limits_{\boldsymbol{y}^L<\boldsymbol{y}<\boldsymbol{y}^U} g(\boldsymbol{x},\boldsymbol{y})\leq 0} \varphi_u(\boldsymbol{u})\, d\boldsymbol{u} \\ P_f^{max} &= \mathbb{P}\left\{\min_{\boldsymbol{y}^L<\boldsymbol{y}<\boldsymbol{y}^U} g(\boldsymbol{x},\boldsymbol{y}) \leq 0\right\} = \int_{\min\limits_{\boldsymbol{y}^L<\boldsymbol{y}<\boldsymbol{y}^U} g(\boldsymbol{x},\boldsymbol{y})\leq 0} \varphi_u(\boldsymbol{u})\, d\boldsymbol{u}, \end{aligned} \tag{3}$$

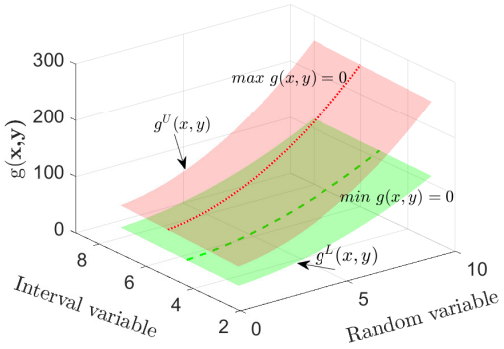

Figure 1: Schematic representation of HRA

where P_f^{min} is the minimum failure probability corresponding to the maximum performance function over the interval uncertainty. In addition, P_f^{max} denotes maximum failure probability due to minimum performance function. $\varphi_u(.)$ describes the joint PDF of independent standard normal random variables (u_i), based on which the individual random variables (x_i) are defined as:

$$x_i = F_{x_i|y}^{-1}(\Phi(u_i)), \quad i = 1, 2, ..., n, \tag{4}$$

where $F_{x_i|y}^{-1}(.)$ is the inverse of marginal CDF of x_i and $\Phi(.)$ refers to the CDF of a u_i. Generally, HRA-IR requires two loops known as inner and outer loops. In the former, minimum/maximum response function with respect to interval variables $\mathbf{y}$ is found and then the failure probability is estimated in the latter. In this context, upper and lower bounds of failure probability $\left[P_f^L, P_f^U\right]$ can be estimated via different reliability methods. In Section 5, an accurate and efficient UQ framework to approximate the P_f^L and P_f^U will be presented.

3. High dimension model representation

High dimensional model representation (HDMR) tools have received attention to approximate expensive-to-evaluate problems with plenty of input parameters with inexpensive-but-accurate metamodels. In other words, the core idea behind HDMR is to find an affordable, yet accurate, input-output mapping derived from the original model. In general, there exist two groups of HDMR expansions namely cut- and random sampling (RS)-HDMR. The former defines the model in reference to a specified cut point in the domain, whereas the latter relies on the mean value of model over the whole domain [48]. This study utilizes the cut-HDMR decomposition with first-order truncation.

3.1. Univariate dimension reduction (UDR) method

Univariate dimension reduction method (UDR) was proposed by Rahman [45]. The main task of UDR is to transform a multi-dimensional response function into multiple one-dimensional functions to compute the statistical moments. Within the arithmetic moments, the response function, $g(\boldsymbol{x})$, is estimated into N (number of variables) one-dimensional functions employing an additive decomposition approach. Then the original N-dimensional integral of the statistical moment is replaced by a number of one-dimensional integrals to enhance the computational efficiency[44]. Moreover, UDR can accurately estimate the statistical moments of the performance function of design variables with both non-normal and normal distributions [49]. On the negative side, the UDR is not recommended for highly nonlinear LSFs and high-dimensional problems. Therefore, the UDR may fail to accurately predict the bounds of intervals for the mentioned complex problems. The a^{th} statistical moment of the $g(\boldsymbol{x})$ can be computed with the following integration [44]:

$$\mathbb{E}\left[g^a(\boldsymbol{x})\right] = \int \cdots \int g^a(x_1, x_2, ..., x_N) f_x(x_1, x_2, ..., x_N) dx_1 dx_2 ... dx_N, \quad a = 0, 1, 2, .., \tag{5}$$

where a is the order of the moment and f_x is a joint probability density function (PDF) of the random parameter $\boldsymbol{x}$. Actually, it is impractical to compute the statistical moments of the performance function using Eq. 5 especially for high dimensional problems. To approximate $g(\boldsymbol{x})$, additive decomposition concept is utilized:

$$g(\boldsymbol{x}) \cong \hat{g}(\boldsymbol{x}) \equiv \sum_{i=1}^{n} g(\mu_1, ..., \mu_{i-1}, x_i, \mu_{i+1}, ..., \mu_n) - (n-1)g(\mu_1, \mu_2, , ..., \mu_n), \tag{6}$$

where $\mu = [\mu_1, \mu_2, \ldots, \mu_n]^T$ is vector of mean value for random variables. For example, the performance function of two-dimension problem is estimated as follows:

$$g(\boldsymbol{x}) \cong \hat{g}(\boldsymbol{x}) \equiv g(x_1, \mu_2) + g(\mu_1, x_2) - g(\mu_1, \mu_2). \tag{7}$$

Frequently, UDR uses $2N+1$ or $4N+1$ axial sampling points to approximate the performance function. It should be mentioned, $4N+1$ sampling points are recommended to use for highly nonlinear problems [50]. Figure 2 shows 2D and 3D problems with $2N+1$ and $4N+1$ axial sampling points. Choosing $2N+1$ or $4N+1$ axial sampling points depends on the level of the nonlinearity of the problem.

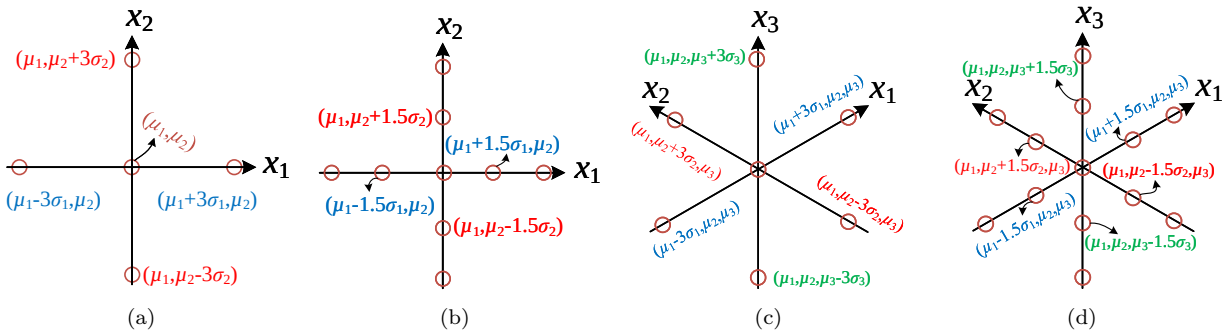

Figure 2: 2D and 3D axial design of experiments (DOEs) via $(2N+1)$ and $(4N+1)$ points

3.2. Numerical interpolation to approximate the response function

To approximate the response function, numerical interpolation methods can map a high-dimensional function to a problem with a desired target dimension, and then generate data from the mapped function at a quite low computational expense [51]. The univariate component function in Eq. 6 can be estimated with function values at a set of univariate sample points as follow [52]:

$$g(\boldsymbol{x}) = g(\mu_1, ..., \mu_{i-1}, x_i, \mu_{i+1}, ..., \mu_n) = \sum_{j=1}^{m} a_j(X_i).g(\mu_1, ..., \mu_{i-1}, x_i^{(j)}, \mu_{i+1}, ..., \mu_n), \tag{8}$$

where m refers to the size of univariate sample $(x_i^{(1)}, x_i^{(2)}, \ldots, x_i^{(m)})$. The function $a_j(X_i)$ indicates the jth interpolation basis function which is named Lagrange polynomial. The function $a_j(X_i)$ has a form in Lagrange interpolation as:

$$a_j(X_i) = \frac{\prod_{k=1,k\neq j}^{m}(X_i - x_i^{(k)})}{\prod_{k=1,k\neq j}^{m}(x_i^{(j)} - x_i^{(k)})}. \tag{9}$$

By applying interpolation for all univariate component functions, an explicit function approximation is provided for the response function:

$$g(\boldsymbol{x}) = \sum_{i=1}^{N}\sum_{j=1}^{m} a_j(X_i).G(\mu_1, ..., \mu_{i-1}, x_i^{(j)}, \mu_{i+1}, ..., \mu_n) - (N-1)G(\boldsymbol{\mu}). \tag{10}$$

If the same size of sample points m is considered for the Lagrange interpolation of all univariate component

functions, therefore $(m-1)N+1$ function evaluations are required for the UDR. Conforming the mentioned process, Lagrange interpolation can be used for the UDR with two or higher-order component functions.

4. Soft Monte Carlo method

The crude MCS is a robust and simple method to estimate the failure probability of complex systems. However, since this approach requires many simulations to approximate the failure probability, it is not the best candidate for the reliability analysis of problems with small failure probabilities. To improve the efficiency of the crude MCS for small failure probabilities, soft Monte Carlo (SMC) is proposed which mathematically provides a general accuracy identical to crude MCS [43]. The main idea of the proposed method, that can be seen as a generalized version of the Line sampling (LS) methodology [53, 54], is to generate a few random PDFs as an alternative to a huge number of random samples. This approach presents suitable flexibilities in probability estimation shown in Ref. [21], that the well-known LS and FORM are a special case of this method. To estimate probabilities by soft MCS approach, 1-D random PDFs should be generated in the u-space based on the joint PDF of random variables. Each 1-D PDF consists of two main features: random location and direction. By generating a typical random sample $\boldsymbol{u}'$, a random direction for the 1-D PDF in u-space can be presented as $\boldsymbol{\alpha} = \boldsymbol{u}'/\left\|\boldsymbol{u}'/\right\|$ [43]. Here, a line that connects origin to the sample $\boldsymbol{u}'$ represents the direction of sampline. Accordingly, the random direction $\boldsymbol{\alpha}$ should be transferred to a random location $\boldsymbol{u}$ (by generating a new random sample in the standard normal space). For the proposed generated random line, the support point (which is the mean point of 1-D random PDF) is determined to be the shortest sampline distance from the origin which reads:

$$\boldsymbol{u}_{sp} = \boldsymbol{x} - \langle \boldsymbol{u}, \boldsymbol{\alpha} \rangle .\boldsymbol{\alpha}, \tag{11}$$

where $\boldsymbol{u}_{sp}$ refers to the location of support point. Here, considering the random PDF as a 1-D local coordinate, the axis (u'') is called "sampline" and the failure probability for the obtained 1-D problem can be estimated as $\hat{P}_f = \int I_g(u'')\,\phi(u'')\,du''$ where I_g is the indicator function. Once several random PDFs are generated in u-space, Eq. 1 estimates the failure probability of the problem as follow:

$$\begin{aligned} &\hat{P}_f = \int I_g(u'')\,\phi(u'')\,du'', \\ &\mathbb{E}(P_f) = \mathbb{E}(\hat{P}_f), \\ &P_f = \mathbb{E}(\hat{P}_f), \end{aligned} \tag{12}$$

where $\hat{P}_f$ is the estimated failure probability for generated 1-D PDFs. The main feature of this approach is that any favorite 1-D integration method can be used to estimate the one-variable integral $\hat{P}_f = \int I_g(u'')\,\phi(u'')\,du''$, while the result has the accuracy as same as the crude MCS. Figure 3 illustrates different strategies of the soft MCS and crude MCS for solving a rare-event problem.

5. Proposed approach

5.1. Soft MCS-based hybrid reliability analysis

In this section, we propose a robust solution for application of soft MCS in hybrid reliability analysis. By employing random PDFs in the simulation process, we present a hybrid reliability problem into two spaces, namely; random space, and optimization space in which the former is used to draw random PDFs from random variables in u-space while the latter is utilized to determine the bounds of preference function for the generated PDFs using interval variables. According to the proposed approach, once a random sampline is generated in random space, its probability bounds can be estimated as 1-D reliability problem with local axis u'' follows:

$$\begin{aligned} \hat{P}_f^{min} &= \mathbb{P}\left\{ \max_{\boldsymbol{y}^L < \boldsymbol{y} < \boldsymbol{y}^U} g(u'') \le 0 \right\} = \int_{\max\limits_{y^L < y < y^U} g(u'') \le 0} \varphi_{u''}(u'')\,du'', \\ \hat{P}_f^{max} &= \mathbb{P}\left\{ \min_{\boldsymbol{y}^L < \boldsymbol{y} < \boldsymbol{y}^U} g(u'') \le 0 \right\} = \int_{\min\limits_{y^L < y < y^U} g(u'') \le 0} \varphi_{u''}(u'')\,du'', \end{aligned} \tag{13}$$

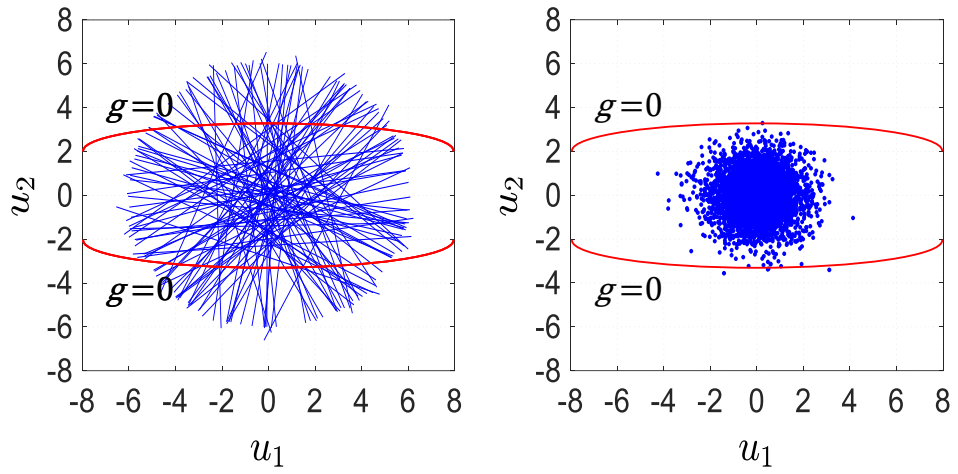

(a) Soft MCS (b) MCS

Figure 3: Comparison between the performance of Soft-MCS and crude MCS via solving rare event problem

where the location of a point on local coordinate u'' can be presented in global coordinate ($\boldsymbol{u}_{Gb}$) as:

$$\boldsymbol{u}_{Gb} = \boldsymbol{u}_{sp} + u''.\boldsymbol{\alpha}. \tag{14}$$

Therefore, the performance function for a point in local coordinate $g(u'')$ can be estimated from global coordinate as $g(\boldsymbol{u}_{Gb}) = g(\boldsymbol{u}_{sp} + u''.\boldsymbol{\alpha})$.
Estimating the probability bounds of sufficient randomly generated samplines in random space, the probability bounds of the problem then can be estimated as follows:

$$\begin{aligned} P_f^{min} &= \mathbb{E}(\hat{P}_f^{min}), \\ P_f^{max} &= \mathbb{E}(\hat{P}_f^{max}). \end{aligned} \tag{15}$$

For estimating the probability bounds of a generated sampline (estimating Eq. 13), the maximum/minimum values of performance function, $g^U = \underset{\boldsymbol{y}\in\boldsymbol{y}^I}{argmax}\,(g(u'', \boldsymbol{y}))$ or $g^L = \underset{\boldsymbol{y}\in\boldsymbol{y}^I}{argmin}\,(g(u'', \boldsymbol{y}))$, should be assessable for each desired point on the sampline. To meet this aim, this study suggests to create optimization space consist of interval variables ($\boldsymbol{y}$) and adding the axis of random PDF (u'': sampline) as an extra dimension to interval variables. As a result, considering reliability problem involving n random variables ($\mathbf{X}$: aleatory variables) and m interval variables ($\boldsymbol{y}$), the proposed random space and optimization space would be n and $m+1$ dimensional spaces, respectively. The proposed implementations are illustrated in Figure 4 for a reliability problem with two random variables ($n = 2$) and one interval variable ($m = 1$).

5.2. Metamodel-based hybrid reliability analysis

To reduce the computational burden of analysis in both reliability and optimization spaces, any desired metamodels can be used for analysis. Nonetheless, this paper suggested application of univariate dimension reduction (UDR) method in analysis that is fit to reduce the computational costs in soft MCS-based reliability analysis.

To accelerate the engine of optimization phase, only few DOEs are required to be located on the axis of random PDF and interval variable axes (See Figure 2). Hence, the performance function for each desired point in optimization process can be predicated as Eq. 10 in which the position of each DOE on the sampline can be determined as $x''_{DOE} = \mu_{n+1} \pm \boldsymbol{r}\sigma = u_{sp} \pm \alpha\boldsymbol{r}\sigma$ where $\boldsymbol{r} = [r_1, r_2, \ldots, r_k]$. r_i is the distance of DOEs from u_{sp} and parameter σ equals 1.0 which is the standard deviation of standard normal PDF.

According to the proposed approach, once the location of x''_{DOE} being determined and UDR-based metamodel formed, the bounds of the performance functions (g^L and g^U) can be determined for each point on the sampline g^L =argmin$(g(u'', \boldsymbol{y}))$ and g^U =argmax$(g(u'', \boldsymbol{y}))$. Using the proposed approach, the total

function calls of method for each sampline would be $(k-1)\times n+1$ where k is the number of DOEs on each axis.

To ease the comprehension of the proposed approach for HRA, in the following, the required steps of the proposed approach for a problem with two random variables, u'', $(n = 2)$ in random space and one interval variable $(m = 1)$ in optimization space are provided in the following:

1. Generating a random PDF (sampline), u'', in the random space as a random variable (RV) using soft MCS method (See Figure 4(a)) and drawing one interval variable in optimization space in Figure 4(b).

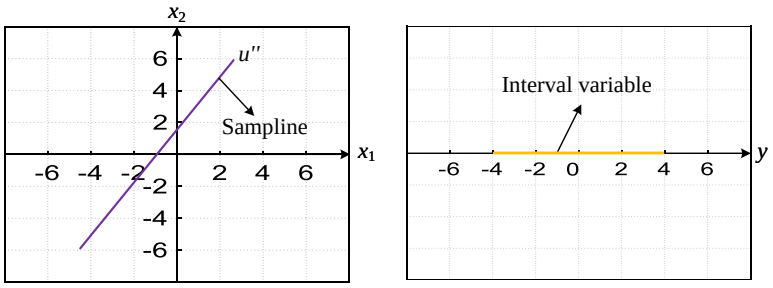

(a) 2-D random variable (u'') in random space

(b) One interval variable in optimization space

Figure 4: Illustration samples in reliability and optimization spaces

2. Adding the sampline, u'', in the optimization space as a new dimension to the interval variable (See Figure 5). The location of mid-point (μ_1, μ_2) is shown in this Figure.

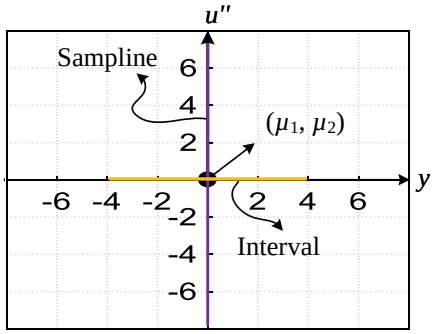

Figure 5: Adding sampline (u'') as a new dimension to interval variables in optimization spaces

3. The DOEs are added to optimization space according to Section 3.1. It should be mentioned that the number of DOEs in the interval variables is taken $2N + 1$ samples (See Figure 6). (Note: The number of DOEs should be considered odd numbers.)

4. Constructing UDR metamodel to predict the g^L =argmin$(g(u'', \boldsymbol{y}))$ and g^U =argmax$(g(u'', \boldsymbol{y}))$ for each samples on sampline x''_{DOE}. In this step, instead of employing original performance function, the proposed surrogate model UDR can be applied in analysis. In fact, we do the 1-D optimization in each blue line. The desired line is shown with a red box in the Figure 7 in form of 2D and 3D plots. In the next step, the continuing process is explained on the desired line.

5. The minimum and maximum values of performance function should be determined in this step, noting that instead of calculating the original performance function, the developed surrogate model of previous step can be used in analysis. Here, as an alternative to using an optimization algorithm (that may fail in local optima), in this step many samples on the desired lines are generated and UDR can be employed to predict the value of performance function for samples on blue lines (See Figure 8).

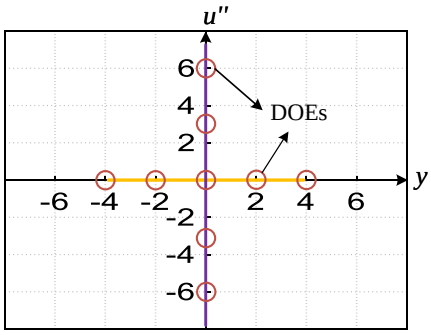

Figure 6: Adding DOEs on the optimization space according to UDR method

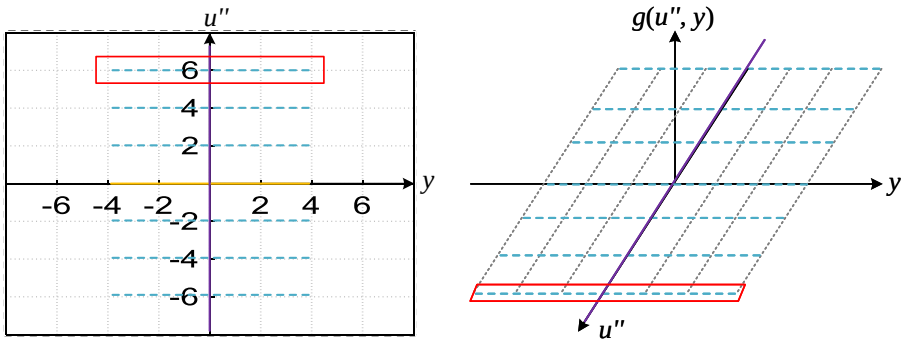

(a) 2D optimization space (b) 3D optimization space

Figure 7: Constructing UDR method to predict the minimum and maximum of performance function on optimization space

Then, minimum and maximum values of predicted performance function, $g^L = argmin(g(\boldsymbol{x}, \mathbf{y}))$ and $g^U = argmax(g(\boldsymbol{x}, \mathbf{y}))$, for each sample on the red line are calculated. For the case of problems with many interval variables (a high dimension search space), the obtained solution may be used as the initial search point and a local search optimization can be performed to achieve more accurate results.

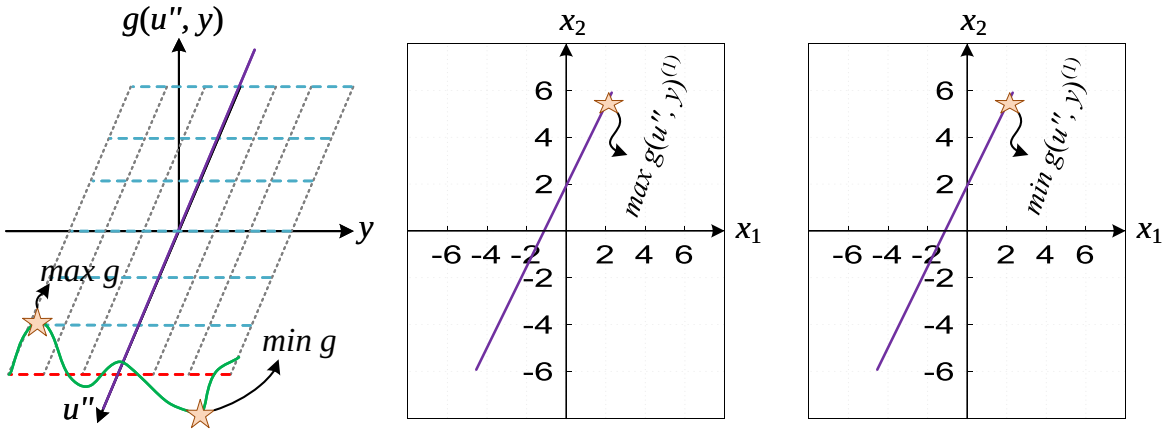

(a) Finding the minimum and maximum values of performance function on desired line in optimization space

(b) Representing the maximum value of performance function on sampline in random space

(c) Representing the minimum value of performance function on sampline in random space

Figure 8: Finding the minimum and maximum values of performance function using UDR for the first desired line in optimization space)

6. Repeating the previous step for the second line in optimization space. For each sampline this process is done to determine the $\hat{P}_f^{min}$ and $\hat{P}_f^{max}$ for that sampline. Finally, the upper and lower bounds of failure probability, P_f^{max} and P_f^{min}, are computed as the mathematical expectation of the obtained probability bounds ($\hat{P}_f^{min}$ and $\hat{P}_f^{max}$) for 1-D coordinates based on Eq. 15.

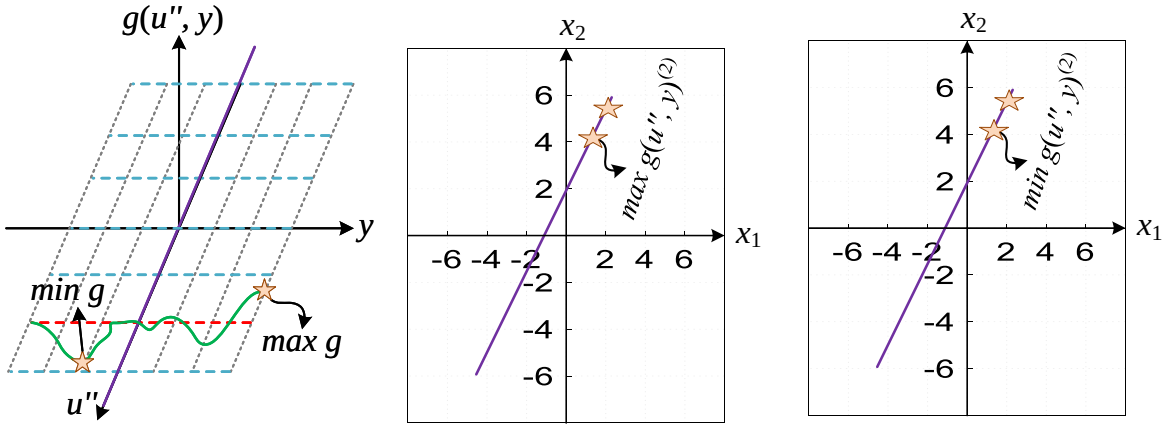

(a) Find minimum and maximum value of performance function on desired line in optimization space

(b) Represent maximum value of performance function on sampline in random space

(c) Represent minimum value of performance function on sampline in random space

Figure 9: Finding the minimum and maximum value of performance function using UDR (Second line)

7. After computing the lower and upper bounds of failure probability, the predefined convergence criteria, assumed to be number of samplines N_{SLine}, should be check. If the desired convergence criteria are satisfied, we can stop algorithm; else, go to step 1. Figure 10 graphically summarizes the steps necessitated for the proposed HRA method, SMC-UDR.

6. Numerical Examples

In this section, two numerical examples and one real-world engineering application, a reinforced concrete (RC) column, are employed to assess the efficiency and accuracy of proposed method. In example 1, a nonlinear performance function is considered with two random variables and one interval variable. In the second example, a roof structure is presented. To verify the performance of SMC-UDR method, it is compared with MCS, FORM-UUA in terms of efficiency and accuracy. For both mathematical examples, the SMC-UDR results are presented for 50 replicants. To extend the application of our proposed method to real-world engineering examples, an RC column also is studied.

6.1. Example 1-A mathematical example

A nonlinear performance function is given as [22, 37]:

$$g(\boldsymbol{x}, \boldsymbol{y}) = sin(\frac{5x_1}{2}) - \frac{(x_1^2+4)(x_2-1)}{20} + y \tag{16}$$

where x_1 and x_2 are random and independent normal variables, i.e, $x_1 \sim N(\mu = 1.5, \sigma = 1)$ and $x_2 \sim N(\mu = 2.5, \sigma = 1)$. y is an interval variable within the region $y \in [2\ , 2.5]$. Table 2 shows the HRA-RI results for MCS, FORM-UUA and SMC-UDR. To estimate the upper and lower bounds of reliability index $\left[\beta^{min},\ \beta^{max}\right]$, MCS requires 2×10^8 function calls (N_{call}) where 200 samples are used for obtaining the minimum and maximum of performance function over the interval variable and 10^6 samples are provided according to the distribution for random variables [22]. The upper and lower bounds of reliability index for MCS are achieved 2.56 and 1.86, respectively. The relative errors, $\varepsilon\left(\beta^{min}\right)$ and $\varepsilon(\beta^{max})$, in comparison

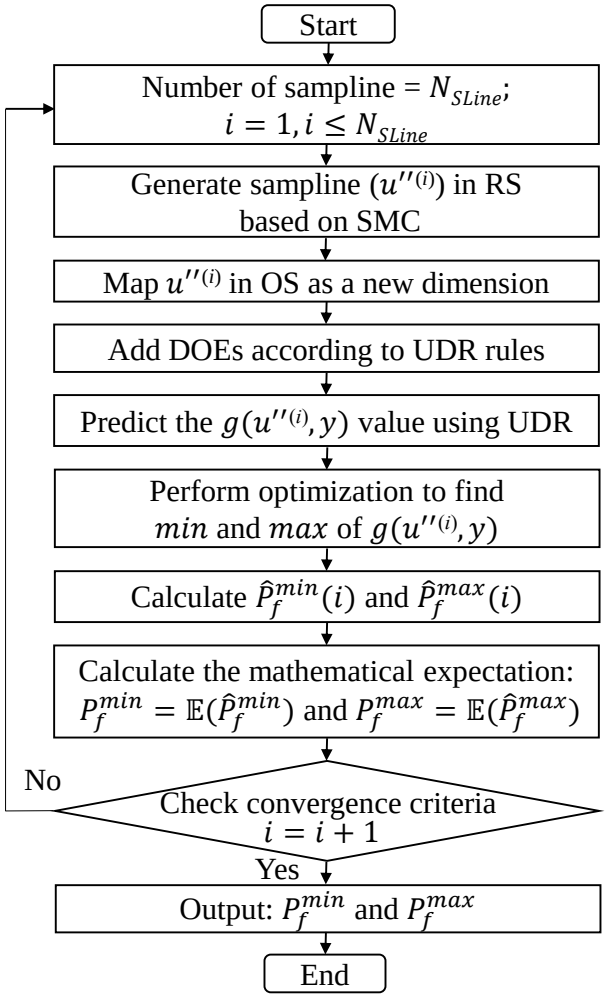

Figure 10: The flowchart of the proposed HRA method (SMC-UDR)

MCS are obtained for FORM-UUA and SMC-UDR.

The SMC-UDR results in Table 2 are the average of 50 independent runs. According to Table 2, the upper and lower bounds of reliability index are obtained by the SMC-UDR 2.50 and 1.85, with the relative errors of 0.023 and 0.005, respectively. In the SMC-UDR, only 10 samplines with 19 DOEs are considered to approximate β^{min} and β^{max}. Thus, the N_{call} for SMC-UDR is 190. To capture the effect of using different seed numbers, this example is replicated 20 times and the coefficient of variations (COVs) for lower and upper bounds are calculated about 0.084 and 0.11, respectively.

The minimum and maximum reliability index via FORM-UUA are obtained 1.18 and 2.40, respectively where FORM-UUA used 1555 samples for HRA-RI. The accuracy of FORM-UUA in the estimation of reliability index is not acceptable in this example. According Table 2, the relative errors for SMC-UDR are smaller than FORM-UUA. Therefore, it confirms that the performance of SMC-UDR is very close to the MCS in this example.

Table 2: Comparison between the performance of three applied HRA-RI approaches for example 1- Scenario I

Method	β^{min}	β^{max}	$\varepsilon(\beta^{min})$	$\varepsilon(\beta^{max})$	N_{call}
MCS+Optimization [22]	1.86	2.56	-	-	2×10^8
FORM-UUA [22]	1.18	2.40	0.366	0.063	1555
SMC-UDR	1.85	2.50	0.005	0.023	190

On the other hand, to demonstrate the role of having intervals with wider bounds, we added another

hypothetical modification named scenario II in which the bounds are artificially increased to [2, 3] and [2 , 4] for case A and B, respectively, in Table 3. As can be seen, the proposed SMC-UDR method can dramatically reduce the computational burden without compromising accuracy in both cases.

Table 3: Comparing the performance of the reference and proposed HRA methods for the artificially increased bounds of the interval variable in example 1 problem, scenario II

Method	β^{min}	β^{max}	$\varepsilon\left(\beta^{min}\right)$	$\varepsilon\left(\beta^{max}\right)$	N_{call}	Case
MCS+Optimization	1.86	2.78	-	-	2×10^6	A
MCS+Optimization	1.86	3.22	-	-	2×10^6	B
SMC-UDR	1.82	2.74	0.02	0.014	190	A
SMC-UDR	1.86	3.29	0.0	0.0217	190	B

6.2. Example 2-A roof truss structure

A roof truss structure is evaluated in this example as shown in Figure 11. The top boom and compression bars are reinforced by concrete. The bottom boom and the tension bars are made by steel. The truss roof is subjected to distributed load q uniformly. The vertical deflection at point C can be computed as [22, 31]:

$$\Delta_C = \frac{ql^2}{2}\left(\frac{3.81}{A_c E_c} + \frac{1.13}{A_s E_s}\right), \tag{17}$$

where E_c and E_s are the Young's moduli of concrete and steel bars, respectively. A_c and A_s represent their cross-sectional areas, respectively. The vertical deflection at node C is limited to 0.025m. The performance function for this structure is considered as $g\left(\boldsymbol{x}, \boldsymbol{y}\right) = 0.025 - \Delta_C$. The random and interval variables for this performance function are listed in Table 4.

In this case study, the cross-sectional areas of the concrete A_c and steel bars A_s are modelled as interval-valued parameters to represent the geometrical tolerances that result from the respective casting processes. Within these tolerance bounds, we do not know the accurate values of A_c and A_s. In fact, we only know them to be located in a certain range, e.g., $A_c = [0.0330.035]$ and A_s=$[9.3 \times 10^{-4}\ 9.5 \times 10^{-4}]$). Accordingly, rather than assuming A_c and A_s to be random variables, it is more appealing to treat them as interval variables, since modeling the pure lack of knowledge and having tolerances on the dimensions as a result of the casting process by intervals is closer to the actual nature of the uncertainty.

In Table 5, the HRA-RI results of MCS, FORM-UUA and SMC-UDR are presented for truss structure. MCS estimates the upper and lower bounds of reliability index 2.09 and 2.39 using 2×10^8 function calls, respectively [22]. In MCS method, 200 samples are drawn for obtaining the minimum and maximum of performance function over the interval variable and 10^6 samples are provided according to the distribution for random variables. FORM-UUA estimates β^{min} and β^{max} in an efficient, yet inaccurate way in comparison MCS. The β^{min} and β^{max} values are achieved approximately 2.07 and 2.39 by SMC-UDR employing 20 samplines.

As a sidenote, it should be pointed out that the interval [2.07 2.39] is more to be regarded as a measure for the sensitivity of our probabilistic computation of the reliability index to the epistemic uncertainty that is present in the system [20]. In this example, since the the interval is comparatively wide, what it actually tells us is that the reliability index that we are computing is very sensitive to the epistemic uncertainty we are faced with. This, in its turn, in practice guides us to collecting more information as to reduce the epistemic uncertainty in the system. Practically speaking, in this case specifically, the recommendation is to either control the casting process such that the tolerances are finer, or to invest in post-casting quality control with sufficiently high resolution.

In SMC-UDR method, the relative errors for the upper and lower bounds of reliability index are obtained 0.0 and 0.01, respectively. In Figure 12, the curve of convergency for the proposed method respect to different number of samplines [10:110] are depicted. After 30 samplines, the SMC-UDR converges to MCS reliability indexes. According to Table 5, the relative errors of SMC-UDR to estimate the upper and lower bound of reliability index are lower than FORM-UUA. Thus, the proposed HRA-RI method outperforms in comparison to other state-of-the-art approaches in terms of efficiency and accuracy. Similar to example 1 with 20 replications, the COVs for lower and upper bounds are obtained about 0.078 and 0.066, respectively.

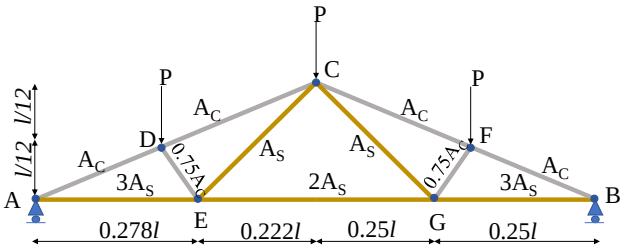

Figure 11: Schematic view of the roof truss structure

Table 4: Random and interval variables for truss structure

Variable	Distribution	Parameter 1	Parameter 2
l[m]	Normal	$\mu = 12$	$\sigma = 0.24$
$E_s[N/m^2]$	Normal	$\mu = 1.2 \times 10^{11}$	$\sigma = 8.4 \times 10^9$
$E_c[N/m^2]$	Normal	$\mu = 3 \times 10^{10}$	$\sigma = 2.4 \times 10^9$
$A_s[m^2]$	Interval	$A_s^L = 9.3 \times 10^{-4}$	$A_s^U = 9.5 \times 10^{-4}$
$A_c[m^2]$	Interval	$A_c^L = 0.033$	$A_c^U = 0.035$

Table 5: HRA-RI results for truss structure

Method	β^{min}	β^{max}	$\varepsilon(\beta^{min})$	$\varepsilon(\beta^{max})$	N_{call}
MCS+Optimization	2.09	2.39	-	-	2×10^8
FORM-UUA	2.6	3.01	0.244	0.259	227+227
SMC-UDR	2.07	2.39	0.01	0	1140

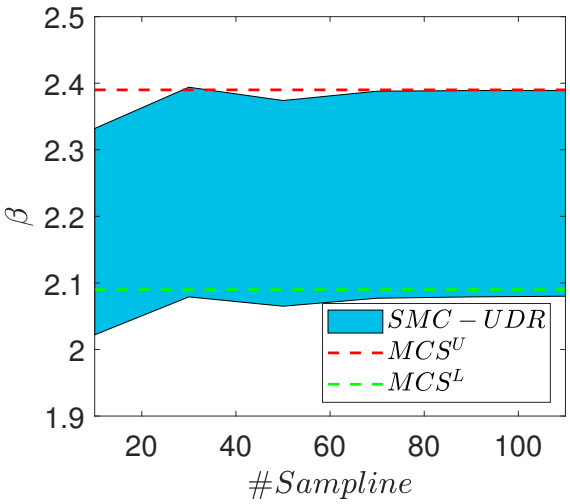

Figure 12: Convergence curve for SMC-UDR

6.3. Application of SMC-UDR in RC columns

Reinforced concrete column is addressed to examine the robustness of HRA-RI for solving real-word structural problems. The focus here is only on the RC short column and the effect of column slenderness is not taken into account in this analysis. Figure 13 shows the cross-section of a circular RC column with five reinforcement layers and a hypothetical strain distribution. Layer 1, with strain ε_{s1}, area A_{s1} and distance d_1 from the extreme compression, is closest to the minimum compression and layers i with strain ε_{si}, area A_{si} is at distances d_i. The strain distribution is defined by setting the maximum strain of concrete $\varepsilon_{cu} = 0.003$ and assuming a value for $\lambda\,(\varepsilon_{s1} = \lambda\varepsilon_y)$, where the positive and negative values of λ correspond, respectively, to the compression and tension stresses in layer 1, and the balanced failure conditions correspond to $\lambda = -1.0$. For each given strain distribution, the nominal axial-force capacity (P_n) can be found as follows:

$$P_n = 0.85 f'_c A_c + \sum_{i=1}^{5} F_{si}, \tag{18}$$

where f'_c is the specified concrete strength in compression, $A_c = \frac{D^2}{4}(\theta - sin\theta cos\theta)$ is the area of the compressive zone of concrete with height a in the circular section (Figure 13) and F_{si} is the force corresponding to the i^{th} reinforcement layer:

$$F_{si} = \begin{cases} f_{si} A_{si}, & a < d_i \\ (f_{si} - 0.85 f'_c) A_{si}, & a \geq d_i, \end{cases} \tag{19}$$

f_{si} is stress in the ith reinforcement layer: $f_{si} = E_s \varepsilon_{si}$ for $|\varepsilon_{si}| < \varepsilon_y$ and $f_{si} = f_y$ for $|\varepsilon_{si}| \geq \varepsilon_y$, where f_y

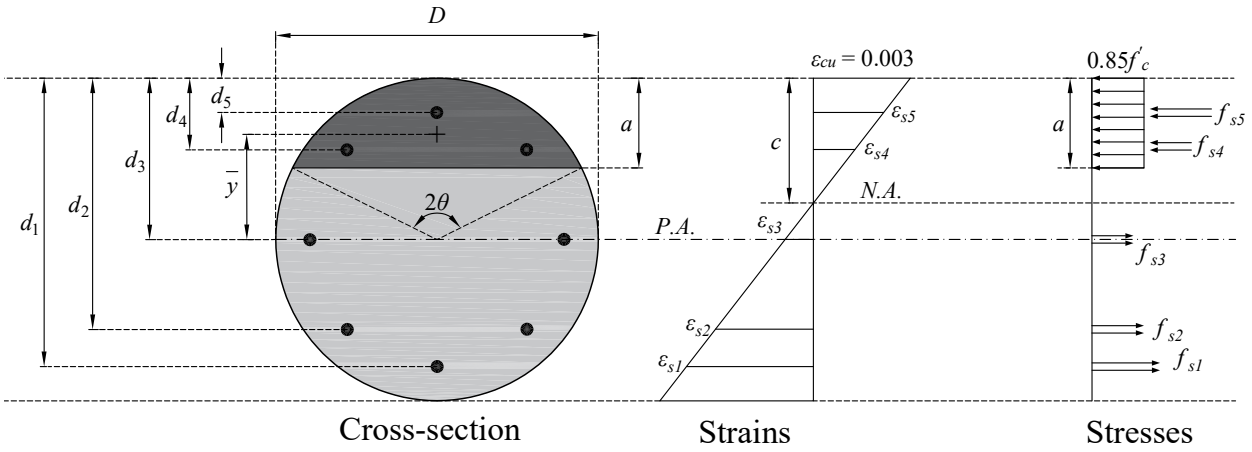

Figure 13: Cross-section of the circular RC column with the distribution of strains and stresses

and ε_y are the steel yield stress and yield strain, respectively, and E_s is the modulus of elasticity. ε_{si} and the depth of the neutral axis c for a given strain distribution are calculated as:

$$\begin{aligned} \varepsilon_{si} &= \left(\tfrac{c - d_i}{c}\right) 0.003, \\ c &= \left(\tfrac{0.003}{0.003 - \lambda \varepsilon_y}\right) d_1. \end{aligned} \tag{20}$$

The nominal bending moment capacity (M_n) of the RC column for the assumed strain distribution can be computed with the following equation:

$$\begin{aligned} M_n &= 0.85 f'_c A_c \bar{y} + \textstyle\sum_{i=1}^{n} F_{si} \, (0.5D - d_i), \\ \bar{y} &= \tfrac{(D sin\theta)^3}{12 A_c}, \end{aligned} \tag{21}$$

where $\bar{y}$ is the distance of the centroid of A_c to the center axis of the section and D is the diameter of the cross-section. In accordance with ACI 318-14 [55], it is necessary that $(\varphi P_n \, , \varphi M_n) \geq (P_u \, , \, M_u)$ where P_u is the factored load, M_u is the factored moment and φ is the strength reduction factor that depends on the failure type, and is considered based on Ref.[55]. P_u and M_u are calculated as [55]:

$$U = max \begin{cases} 1.4DL, \\ 1.2DL + 1.6LL, \end{cases} \tag{22}$$

the DL and LL are dead and live loads,respectively. P_{Dn}, P_{Ln}, M_{Dn} and M_{Ln} are calculated based on $LL/DL = 0.7$ by equating design capacities and load effects, finally, the mean and standard deviation are evaluated for P and M caused by DL and LL . The P and M interaction in the RC column for a set of strain distributions is shown in Figure 14; points inside this diagram, e.g. SP, mean loads less than the section resistance and, therefore, will not cause failure (safe zone), and those outside this diagram, e.g. FP, indicate the failure zone. The performance function $g(\boldsymbol{x})$ of the RC column is formulated based on the interaction

diagram and the factored loads:

$$g(\boldsymbol{x}) = E_R\sqrt{P_R^2(\boldsymbol{x}) + \frac{M_R^2(\boldsymbol{x})}{D}} - \sqrt{P_u^2(\boldsymbol{x}) + \frac{M_u^2(\boldsymbol{x})}{D}}, \tag{23}$$

where are $P_R = \varphi P_n$ and $M_R = \varphi M_n$ are axial and bending strength of RC column and E_R is the resistance modeling error. A normal distribution is used for E_R with a mean of 1.0 ($\mu_{E_R} = 1.0$) and a coefficient of variation of 0.065($COV_{E_R} = 0.065$) for the compression failure range ($C_0 - C_1 - B$ in Figure 14), and $\mu_{E_R} = 1.0$ and $COV_{E_R} = 0.03 + \frac{(0.065-0.03)e_B}{e_i}$ for the transition and tension failure ranges ($B - T_1 - T_0$ in Figure 14), where e_B is the balanced failure-related eccentricity [56, 57].

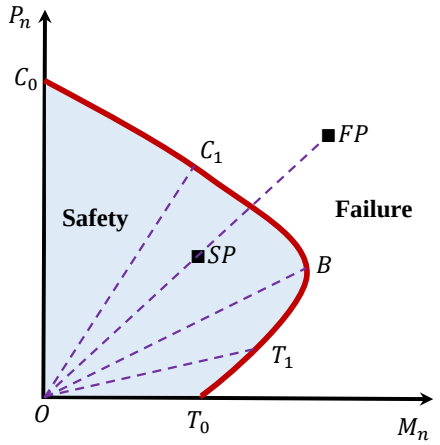

Figure 14: Interaction diagram of the circular RC column

HRA-RI based on SMC-UDR with 40 samplines is used for the circular RC column shown in Figure 15 with the reinforcement ratio $R = 1.7\%$, the probabilistic models in Table 6, and the variable λ in 5 intervals as $I\lambda_1 = (0.21, 0.45)$, $I\lambda_2 = (-0.83, -0.58)$, $I\lambda_3 = (-1.17, -0.98)$, $I\lambda_4 = (-1.45, -1.27)$ and $I\lambda_5 = (-1.96, -1.85)$ which correspond to the eccentricity intervals $IE_1 = (5,\ 30)$, $IE_2 = (105,\ 130)$, $IE_3 = (150,\ 175)$, $IE_4 = (190,\ 215)$ and $IE_5 = (280,\ 305)$ mm, respectively.

In this practical case study, several parameters can be treated as random variables (please refer to Table 6). In parallel, this study suggests that the load eccentricity and reinforcement ratio should be treated as interval variables during the early-stage design of structures. The reasoning for this is the following. During the modeling of the load eccentricity in reinforced concrete structures [58, 55], the only available information in standards is the given 25-millimeter maximum allowable deviation from being plumb. Therefore, this lack of knowledge and source of uncertainty can be captured via interval variables, as opposed to the recommendations for the nominal value representation in design codes.

Moreover, by virtue of the HRA framework to model this parameter as interval, it is possible to study the sensitivity of the P_f estimation on potential mismatches in the eccentricity due to misplacement. Since we do not have any knowledge on the distribution of such misalignment, we opt to use an interval to model the worst and best-case behavior. Accordingly, by considering +25 mm, the eccentricity intervals (IE) are defined. It is worth noting that IE_1 and IE_2 belong to the compression failure zones, and IE_3, and IE_5 refer to the balanced and tension failure zones, respectively. Moreover, IE_4 represents the transition range.

ACI 318-14 [55] recommended that a designer is allowed to design a structure between upper and lower bounds for the reinforcement ratio (R). To capture this source of randomness in early-design phases when no prior knowledge is available, we modeled it by interval variables. In this setting, a designer is allowed to calculate it between upper and lower thresholds. Three different interval ratios (IR) are assumed in this study, namely 1.4, 2.1 and 3.4 with an increase interval of 0.3 for each of which. In this context, the IRs are expressed in a way that the values are within 1.0 and 4.0.

Comparison of HRA-RI results based on SMC-UDR and MCS ($N_{call} = 2 \times 10^8$) in Figure 16 show that β_{min} and β_{max} calculated by SMC-UDR at intervals $I\lambda_1$ and $I\lambda_2$ are very close the MCS results (error less than 0.7%) and the maximum error of β_{min} and β_{max} in the other three ranges of λ are 1.1% ($I\lambda_5$)

and 2.33% ($I\lambda_4$) , respectively. Figure 16 reveal that the interval (β_{min}, β_{max}) shrinking based on both SMC-UDR and MCS as the eccentricity of load changes from $I\lambda_1$ to $I\lambda_5$.

Table 6: Probability models of random variables for the circular RC column

Variable	Distribution	Bias factor	COV	Ref
f_c'=34.5MPa	Normal	1.19	0.135	[59, 60]
f_y=414MPa	Lognormal	1.13	0.03	[59, 60]
E_R[1]	Normal	1.0	0.065	[56, 57]
E_R[2]	Normal	1.0	$0.03+\frac{(0.065-0.03)e_B}{e_i}$	[56, 57]
DL	Normal	1.05	0.1	[59, 61]
LL	Extreme type I	1.0	0.18	[59]

1: Compression failure
2: Tension failure

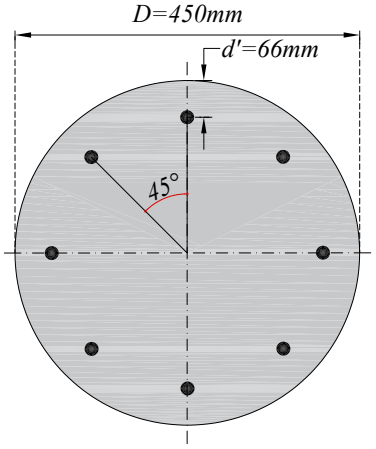

Figure 15: Cross-section of the RC column

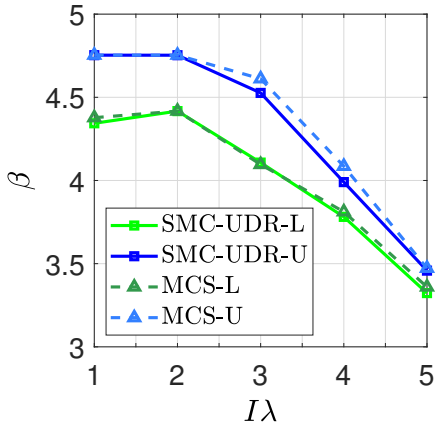

Figure 16: HRA-RI results of the RC column for different intervals of λ.

In another case, HRA-RI is performed for the RC column using SMC-UDR (40 samplines) and MCS ($N_{call} = 2\times10^8$) with probabilistic models in Table 6, variable R in 3 intervals as $IR_1 = (1.4, 1.7)$, $IR_2 = (2.1, 2.4)$ and $IR_3 = (3.5, 3.8)$ percent and variable λ in 5 intervals including $I\lambda_1 = (0.21, 0.45)$, $I\lambda_2 = (-0.83, -0.58)$, $I\lambda_3 = (-1.17, -0.98)$, $I\lambda_4 = (-1.45, -1.27)$ and $I\lambda_5 = (-1.96, -1.85)$. Figure 17 indicated that the maximum error β_{min} and β_{max} based on SMC-UDR are 2.47% ($\beta_{min,IR_3I\lambda_3}$) and 3.08% ($\beta_{max,IR_2I\lambda_3}$), respectively, while the error is less than 0.5% for $\beta_{min,IR_2(I\lambda_3,I\lambda_4,I\lambda_5)}$, $\beta_{min,IR_3(I\lambda_1,I\lambda_2,I\lambda_5)}$, $\beta_{max,IR_1(I\lambda_1,I\lambda_2,I\lambda_5)}$, $\beta_{max,IR_2(I\lambda_1,I\lambda_2)}$ and $\beta_{max,IR_3(I\lambda_1,I\lambda_2,I\lambda_3,I\lambda_4)}$. As shown in Figure 17, increasing the

eccentricity of the load leads to a reduction in β_{min} and β_{max} of the RC column for IR_1, which is significant for $I\lambda_4$ and $I\lambda_5$ while this trend is lower for IR_2 and IR_3 . β_{min} of the circular RC column using SMC-UDR and MCS is 3.1270 and 3.0882 corresponding to $IR_1 I\lambda_5$ while β_{max} based on both SMC-UDR and MCS is 4.7534 corresponding to $IR_1(I\lambda_1,\ I\lambda_2), IR_2(I\lambda_1, I\lambda_2)$ and $IR_3(I\lambda_1, I\lambda_2, I\lambda_3, I\lambda_4)$.

This engineering example illustrates our argument that allocating a probabilistic definition, by using a probability density function for uncertain parameters, when there exists a pure lack of knowledge can lead to misleading judgments. Using intervals, rather, we obtain an objective measure for the effect of the epistemic uncertainty on the probabilistic calculations we are interested in. To put it another way, the interval bounds can serve as a measure for the sensitivity of the reliability index to the epistemic uncertainty. This also can help engineers in the early stage of structural design to make targeted decisions.

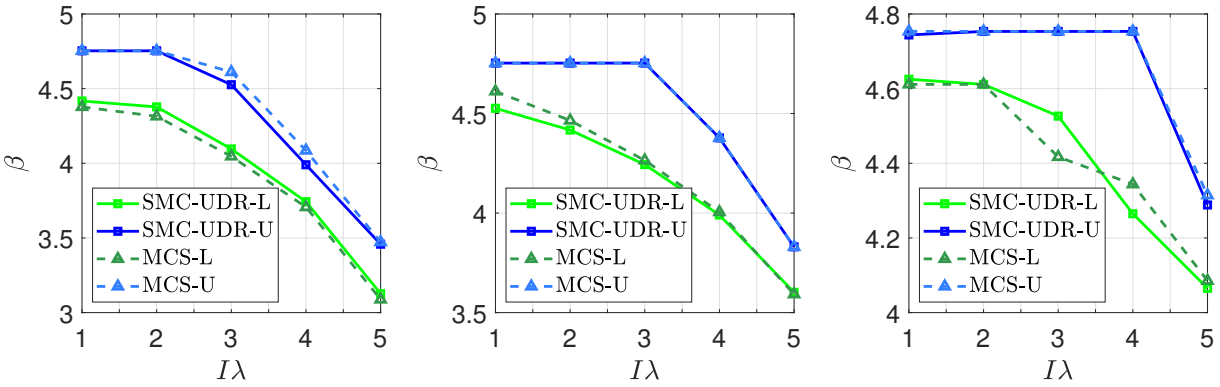

(a) IR1 (b) IR2 (c) IR3

Figure 17: HRA-RI results of the RC column for different intervals of λ and R.

7. Discussion and future study

We should clarify here that, because of application of a metamodel in analysis, the proposed approach is fit to solve only a certain class of problems because: In the optimization phase, for reducing the function calls of analysis, we applied UDR approach that requires very few DOEs to provide a surrogate function for predicting the performance function of the problem. For the problems with highly nonlinear LSF (e.g., the noisy functions), the UDR may present inaccurate prediction at the bounds of intervals. For the case of solved examples, we have used problems with moderate nonlinear performance functions. For the case of very complex problems, more accurate high dimension model representation (HDMR) models such as bi-variate dimension reduction method (BDRM) or other meta models such as Kriging and artificial neural network can be used in analysis. In addition, as it can be seen from the solved examples, the proposed approach works very efficient only for the problems with few random variables. For those including many random variables, many samplines may be required to accurately solve the problem that makes the method inefficient. For reducing the function calls of analysis, we should find the importance failure regions and then, instead of fully random samplines we should use semi-random sampline in analysis (as clarified in the original reference [43]).

Remark 1. If we prevent using a meta model in analyzes (perform global optimization, accurately), we can anticipate accurate results for the problem at the expense of increasing computational costs since the accuracy of soft Monte Carlo is mathematically as same as crude Monte Carlo simulation [43].

Remark 2. Solving problems in the context of probability boxes is an interesting topic for further investigations.

8. Conclusion

This paper proposes a novel hybrid reliability analysis with both random and interval variables (HRA-RI) framework based on coupling soft Monte Carlo simulation and unified dimension reduction methods

(SMC-UDR) to handle hybrid structural reliability problems which deals with random and interval variables concurrently. SMC-UDR is an accurate and efficient UQ methodology to estimate the lower and upper bounds of failure probability. In fact, accuracy is ensured thanks to similar behavior of SMC simulation in comparison to MCS, while efficiency is guaranteed via applying UDR technique which an N-D integral is replaced by an inexpensive-to-evaluate 1-D one. To meet this aim, the proposed HRA-RI framework is presented into two spaces including optimization space and random space. First, the generated 1-D random sampline (i.e, random PDF) in the random space is added to optimization space as a new dimension of interval variable. Second, by adding DOEs in the augmented optimization space, we utilized UDR technique to predict the value of performance function. Third, the minimum and maximum values of performance function are computed to obtain the upper and lower bounds of failure probability. Finally, for each random sampline, this process will be repeated until satisfying the considered criteria. Both accuracy and efficiency of the suggested algorithm are challenged with mathematical and real-world problems.

In this study, the practical need to handle hybrid uncertainties is also scrutinized via the proper classification of interval and random variables based on the nature of real-world engineering problems. Negligible calculated relative errors for both upper and lower bounds of failure probabilities in comparison to other HRA-RI techniques reveals the accuracy of SMC-UDR method. It should be emphasized that because of limitations of the cut-HDMR decomposition approach with first-order truncation, the suggested approach may not be a good alternative for solving high dimensional problems with significant interaction effects among variables.

Acknowledgments

The authors would like to thank the anonymous reviewers for their helpful and constructive comments, which have greatly contributed to improving the final version of this paper.

References

[1] M. Faes, M. Imholz, D. Vandepitte, D. Moens, A review of interval field approaches for uncertainty quantification in numerical models, Modern Trends in Structural and Solid Mechanics 3: Non-deterministic Mechanics (2021) 95–110.

[2] A. Der Kiureghian, O. Ditlevsen, Aleatory or epistemic? does it matter?, Structural safety 31 (2009) 105–112.

[3] N. Metropolis, S. Ulam, The monte carlo method, Journal of the American statistical association 44 (1949) 335–341.

[4] S.-K. Au, J. L. Beck, Estimation of small failure probabilities in high dimensions by subset simulation, Probabilistic engineering mechanics 16 (2001) 263–277.

[5] A. Abdollahi, M. A. Moghaddam, S. A. H. Monfared, M. Rashki, Y. Li, A refined subset simulation for the reliability analysis using the subset control variate, Structural Safety 87 (2020) 102002.

[6] A. Amini, A. Abdollahi, M. A. Hariri-Ardebili, U. Lall, Copula-based reliability and sensitivity analysis of aging dams: Adaptive kriging and polynomial chaos kriging methods, Applied Soft Computing 109 (2021) 107524.

[7] Z. Lu, S. Song, Z. Yue, J. Wang, Reliability sensitivity method by line sampling, Structural Safety 30 (2008) 517–532.

[8] M. Kia, A. Amini, M. Bayat, P. Ziehl, Probabilistic seismic demand analysis of structures using reliability approaches, Journal of Earthquake and Tsunami 15 (2021) 2150011.

[9] M. Beer, S. Ferson, V. Kreinovich, Imprecise probabilities in engineering analyses, Mechanical systems and signal processing 37 (2013) 4–29.

[10] S. Ferson, V. Kreinovich, L. Grinzburg, D. Myers, K. Sentz, Constructing probability boxes and dempster-shafer structures (no. sand-2015-4166j), Sandia National Lab.(SNL-NM), Albuquerque, NM (United States) (2015).

[11] J. Sadeghi, M. De Angelis, E. Patelli, Robust propagation of probability boxes by interval predictor models, Structural Safety 82 (2020) 101889.

[12] M. G. Faes, M. Broggi, G. Chen, K.-K. Phoon, M. Beer, Distribution-free p-box processes based on translation theory: Definition and simulation, Probabilistic Engineering Mechanics 69 (2022) 103287.

[13] Y. Xiang, B. Pan, L. Luo, A sensitivity analysis method to evaluate the impacts of random and interval variables on the probability box, Applied Mathematical Modelling 93 (2021) 538–562.

[14] J. Guo, X. Du, Reliability sensitivity analysis with random and interval variables, International journal for numerical methods in engineering 78 (2009) 1585–1617.

[15] Z. Qiu, J. Wang, The interval estimation of reliability for probabilistic and non-probabilistic hybrid structural system, Engineering Failure Analysis 17 (2010) 1142–1154.

[16] J. Song, P. Wei, M. Valdebenito, S. Bi, M. Broggi, M. Beer, Z. Lei, Generalization of non-intrusive imprecise stochastic simulation for mixed uncertain variables, Mechanical Systems and Signal Processing 134 (2019) 106316.

[17] C. van Mierlo, L. Burmberger, M. Daub, F. Duddeck, M. G. Faes, D. Moens, Interval methods for lack-of-knowledge uncertainty in crash analysis, Mechanical Systems and Signal Processing 168 (2022) 108574.

[18] H.-R. Bae, R. V. Grandhi, R. A. Canfield, An approximation approach for uncertainty quantification using evidence theory, Reliability Engineering & System Safety 86 (2004) 215–225.

[19] P. Huang, H.-Z. Huang, Y.-F. Li, H.-M. Qian, An efficient and robust structural reliability analysis method with mixed variables based on hybrid conjugate gradient direction, International Journal for Numerical Methods in Engineering 122 (2021) 1990–2004.

[20] M. G. Faes, M. Daub, S. Marelli, E. Patelli, M. Beer, Engineering analysis with probability boxes: A review on computational methods, Structural Safety 93 (2021) 102092.

[21] X. Du, Unified uncertainty analysis by the first order reliability method (2008).

[22] J. Zhang, M. Xiao, L. Gao, J. Fu, A novel projection outline based active learning method and its combination with kriging metamodel for hybrid reliability analysis with random and interval variables, Computer methods in applied mechanics and engineering 341 (2018) 32–52.

[23] N.-C. Xiao, H.-Z. Huang, Z. Wang, Y. Liu, X.-L. Zhang, Unified uncertainty analysis by the mean value first order saddlepoint approximation, Structural and Multidisciplinary Optimization 46 (2012) 803–812.

[24] M. G. Faes, M. A. Valdebenito, D. Moens, M. Beer, Bounding the first excursion probability of linear structures subjected to imprecise stochastic loading, Computers & Structures 239 (2020) 106320.

[25] C. Dang, P. Wei, M. G. Faes, M. Beer, Bayesian probabilistic propagation of hybrid uncertainties: Estimation of response expectation function, its variable importance and bounds, Computers & Structures 270 (2022) 106860.

[26] M. G. Faes, M. A. Valdebenito, D. Moens, M. Beer, Operator norm theory as an efficient tool to propagate hybrid uncertainties and calculate imprecise probabilities, Mechanical Systems and Signal Processing 152 (2021) 107482.

[27] P. Ni, D. J. Jerez, V. C. Fragkoulis, M. G. Faes, M. A. Valdebenito, M. Beer, Operator norm-based statistical linearization to bound the first excursion probability of nonlinear structures subjected to imprecise stochastic loading, ASCE-ASME Journal of Risk and Uncertainty in Engineering Systems, Part A: Civil Engineering 8 (2022) 04021086.

[28] P. R. Adduri, R. C. Penmetsa, Bounds on structural system reliability in the presence of interval variables, Computers & structures 85 (2007) 320–329.

[29] X. Du, Interval reliability analysis, in: International Design Engineering Technical Conferences and Computers and Information in Engineering Conference, volume 48078, 2007, pp. 1103–1109.

[30] C. Jiang, G. Lu, X. Han, L. Liu, A new reliability analysis method for uncertain structures with random and interval variables, International Journal of Mechanics and Materials in Design 8 (2012) 169–182.

[31] X. Yang, Y. Liu, Y. Gao, Y. Zhang, Z. Gao, An active learning kriging model for hybrid reliability analysis with both random and interval variables, Structural and Multidisciplinary Optimization 51 (2015) 1003–1016.

[32] S. Xie, B. Pan, X. Du, An efficient hybrid reliability analysis method with random and interval variables, Engineering Optimization 48 (2016) 1459–1473.

[33] B. Bai, W. Zhang, B. Li, C. Li, G. Bai, Application of probabilistic and nonprobabilistic hybrid reliability analysis based on dynamic substructural extremum response surface decoupling method for a blisk of the aeroengine, International Journal of Aerospace Engineering 2017 (2017).

[34] M. Xiao, J. Zhang, L. Gao, S. Lee, A. T. Eshghi, An efficient kriging-based subset simulation method for hybrid reliability analysis under random and interval variables with small failure probability, Structural and Multidisciplinary Optimization 59 (2019) 2077–2092.

[35] W. Wang, H. Xue, T. Kong, An efficient hybrid reliability analysis method for structures involving random and interval variables, Structural and Multidisciplinary Optimization 62 (2020) 159–173.

[36] P. Wang, L. Yang, N. Zhao, L. Li, D. Wang, A new sorm method for structural reliability with hybrid uncertain variables, Applied Sciences 11 (2020) 346.

[37] D. Zhang, S. Liu, J. Wu, Y. Wu, J. Liu, An active learning hybrid reliability method for positioning accuracy of industrial robots, Journal of Mechanical Science and Technology 34 (2020) 3363–3372.

[38] M. Xiao, J. Zhang, L. Gao, A kriging-assisted sampling method for reliability analysis of structures with hybrid uncertainties, Reliability Engineering & System Safety 210 (2021) 107552.

[39] X. Zhang, Z. Wu, H. Ma, M. D. Pandey, An effective kriging-based approximation for structural reliability analysis with random and interval variables, Structural and Multidisciplinary Optimization 63 (2021) 2473–2491.

[40] F. Li, Y. Zhou, T. Wei, H. Li, An interval-probability hybrid reliability method for truck frame, Journal of Failure Analysis and Prevention (2022) 1–8.

[41] X.-Y. Zhou, N.-W. Wang, W. Xiong, W.-Q. Wu, C. Cai, Multi-scale reliability analysis of frp truss bridges with hybrid random and interval uncertainties, Composite Structures 297 (2022) 115928.

[42] D. Bofan, L. Zhenzhou, Efficient adaptive kriging for system reliability analysis with multiple failure modes under random and interval hybrid uncertainty, Chinese Journal of Aeronautics 35 (2022) 333–346.

[43] M. Rashki, The soft monte carlo method, Applied Mathematical Modelling 94 (2021) 558–575.

[44] J. Won, C. Choi, J. Choi, Improved dimension reduction method (drm) in uncertainty analysis using kriging interpolation, Journal of mechanical science and technology 23 (2009) 1249–1260.

[45] S. Rahman, H. Xu, A univariate dimension-reduction method for multi-dimensional integration in stochastic mechanics, Probabilistic Engineering Mechanics 19 (2004) 393–408.

[46] Y. Zhao, J. Yang, M. G. Faes, S. Bi, Y. Wang, The sub-interval similarity: A general uncertainty quantification metric for both stochastic and interval model updating, Mechanical Systems and Signal Processing 178 (2022) 109319.

[47] S. Ferson, W. L. Oberkampf, Validation of imprecise probability models, International Journal of Reliability and Safety 3 (2009) 3–22.

[48] G. Li, S.-W. Wang, C. Rosenthal, H. Rabitz, High dimensional model representations generated from low dimensional data samples. i. mp-cut-hdmr, Journal of Mathematical Chemistry 30 (2001) 1–30.

[49] I. Lee, K. K. Choi, L. Du, Alternative methods for reliability-based robust design optimization including dimension reduction method, in: International Design Engineering Technical Conferences and Computers and Information in Engineering Conference, volume 4255, 2006, pp. 1235–1246.

[50] G. Lee, S. Yook, K. Kang, D.-H. Choi, Reliability-based design optimization using an enhanced dimension reduction method with variable sampling points, International Journal of Precision Engineering and Manufacturing 13 (2012) 1609–1618.

[51] S.-H. Bae, J. Y. Choi, J. Qiu, G. C. Fox, Dimension reduction and visualization of large high-dimensional data via interpolation, in: Proceedings of the 19th ACM international symposium on high performance distributed computing, 2010, pp. 203–214.

[52] C. Hu, B. D. Youn, P. Wang, et al., Engineering design under uncertainty and health prognostics, Springer, 2019.

[53] P.-S. Koutsourelakis, H. J. Pradlwarter, G. I. Schueller, Reliability of structures in high dimensions, part i: algorithms and applications, Probabilistic Engineering Mechanics 19 (2004) 409–417.

[54] P.-S. Koutsourelakis, Reliability of structures in high dimensions. part ii. theoretical validation, Probabilistic engineering mechanics 19 (2004) 419–423.

[55] A. Code, Building code requirements for structural concrete, American Concrete Institute, 2014.

[56] S. A. Mirza, Reliability-based design of reinforced concrete columns, Structural Safety 18 (1996) 179–194.

[57] H. Hong, W. Zhou, Reliability evaluation of rc columns, Journal of Structural Engineering 125 (1999) 784–790.

[58] A. Committee, Specifications for tolerances for concrete construction and materials (aci 117m-10) and commentary, American Concrete Institute, 2010.

[59] A. S. Nowak, K. R. Collins, Reliability of structures, CRC press, 2012.

[60] M. Israel, B. Ellingwood, R. Corotis, Reliability-based code formulations for reinforced concrete buildings, Journal of Structural Engineering 113 (1987) 2235–2252.

[61] H. Shahraki, N. Shabakhty, The seismic performance reliability of reinforced concrete moment structures., Tehnicki vjesnik/Technical Gazette 22 (2015).